



HAL
open science

Plant-wide investigation of sulfur flows in a water resource recovery facility (WRRF)

F. Forouzanmehr, Q.H. Le, K. Solon, V. Maisonnave, O. Daniel, P. Buffiere,
Sylvie Gillot, E.I.P. Volcke

► To cite this version:

F. Forouzanmehr, Q.H. Le, K. Solon, V. Maisonnave, O. Daniel, et al.. Plant-wide investigation of sulfur flows in a water resource recovery facility (WRRF). *Science of the Total Environment*, 2021, 801, pp.149530. 10.1016/j.scitotenv.2021.149530 . hal-03323823

HAL Id: hal-03323823

<https://hal.science/hal-03323823>

Submitted on 20 Sep 2022

HAL is a multi-disciplinary open access archive for the deposit and dissemination of scientific research documents, whether they are published or not. The documents may come from teaching and research institutions in France or abroad, or from public or private research centers.

L'archive ouverte pluridisciplinaire **HAL**, est destinée au dépôt et à la diffusion de documents scientifiques de niveau recherche, publiés ou non, émanant des établissements d'enseignement et de recherche français ou étrangers, des laboratoires publics ou privés.

1 **Plant-wide investigation of sulfur flows in a water resource recovery facility (WRRF)**

2 F. Forouzanmehr ^{a, b, c}, Q. H. Le ^a, K. Solon ^a, V. Maisonnave ^b, O. Daniel ^b, P. Buffiere ^c, S. Gillot ^d, E. I. P. Volcke^{a,*}

3 ^a Department of Green Chemistry and Technology, Ghent University, Belgium

4 ^b Veolia Recherche & Innovation (VeRI), Maisons-Laffitte, France

5 ^c Univ Lyon, INSA-Lyon, Laboratory of Waste Water Environment and Pollutions (DEEP) EA 7429, F-69621
6 Villeurbanne, France

7 ^d INRAE, UR REVERSAAL, F-69625, Villeurbanne Cedex, France

8 * Corresponding author. E-mail address: Eveline.Volcke@UGent.be (E.I.P. Volcke)

9

10 **Abstract**

11 Even though sulfur compounds and their transformations may strongly affect wastewater treatment processes, their
12 importance in water resource recovery facilities (WRRF) operation remains quite unexplored, notably when it comes
13 to full-scale and plant-wide characterization. This contribution presents a first-of-a-kind, plant-wide quantification of
14 total sulfur mass flows for all water and sludge streams in a full-scale WRRF. Because of its important impact on (post-
15 treatment) process operation, the gaseous emission of sulfur as hydrogen sulfide (H₂S) was also included, thus enabling
16 a comprehensive evaluation of sulfur flows. Data availability and quality were optimized by experimental design and
17 data reconciliation, which were applied for the first time to total sulfur flows. Total sulfur flows were successfully
18 balanced over individual process treatment units as well as the plant-wide system with only minor variation to their
19 original values, confirming that total sulfur is a conservative quantity. The two-stage anaerobic digestion with
20 intermediate thermal hydrolysis led to a decreased sulfur content of dewatered sludge (by 36%). Higher (gaseous) H₂S
21 emissions were observed in the second-stage digester (42% of total emission) than in the first one, suggesting an impact
22 of thermal treatment on the production of H₂S. While the majority of sulfur mass flow from the influent left the plant
23 through the treated effluent (> 95%), the sulfur discharge through dewatered sludge and gaseous emissions are critical.
24 The latter are indeed responsible for odour nuisance, lower biogas quality, SO₂ emissions upon sludge combustion and
25 corrosion effects.

26 **Keywords:** *Wastewater treatment, Sulfur mass flows, Experimental design, Plant-wide data analysis, Data*
27 *reconciliation*

28 1. Introduction

29 Wastewater treatment plants (WWTPs) are no longer viewed solely for protecting the aquatic environment and
30 ensuring the required effluent quality in terms of chemical oxygen demand and nutrients (nitrogen and phosphorus),
31 but instead, they are increasingly regarded as water resource recovery facilities (WRRFs) with growing interest for
32 energy and resource recovery (Hao et al., 2019; Solon et al., 2019a). The energy recovery is mostly in the form of
33 methane-containing biogas produced from anaerobic digestion (Guest et al., 2009) that can be combusted on-site for
34 heat and electricity generation or cleaned-up and sold (Puchongkawarin et al., 2015). The resource recovery in WRRFs
35 typically relates to phosphorus and nitrogen recovery which are of the interest due to limited resource of phosphorus
36 and substantial energy requirement for nitrogen production and greenhouse gas emission, respectively (Galloway and
37 Cowling, 2002; Marti et al., 2008; Mihelcic et al., 2011; Puchongkawarin et al., 2015).

38 Sulfur cycle influences both energy recovery and resource recovery, in addition to safety concerns. The methane
39 production can be negatively affected by the competition of sulfate-reducing bacteria and methanogens for hydrogen
40 and acetate (Harada et al., 1994; Muyzer and Stams, 2008; Visser et al., 1993). Moreover, sulfide, especially in un-
41 dissociated form, has an inhibitory effect on anaerobes (e.g. methanogens and acetogens) which are involved in the
42 anaerobic digestion of sludge (Appels et al., 2008; Chen et al., 2008; Guerrero et al., 2016; Yang et al., 2016).
43 Generation of high concentration of hydrogen sulfide (H₂S) in biogas necessitates further processing of biogas before
44 co-generation due to its corrosive properties (Tchobanoglus et al., 2003); hence lowering the profitability of produced
45 biogas.

46 The sulfur cycle is strongly linked to that of other elements such as nitrogen and phosphorus through various biological
47 and (geo)chemical processes (Lomans et al., 2002; Puyol et al., 2017; Solon et al., 2019b). These interactions include
48 the reoxidation of iron sulfide in the aeration tank (Schipper and Jørgensen, 2002) and subsequent precipitation of
49 phosphate with released iron (Ge et al., 2013; Gutierrez et al., 2010), effects on the performance of enhanced biological
50 phosphorus removal (EBPR) process as a result of SRB activity (Baetens et al., 2001; Wanner et al., 1987; Yamamoto-
51 Ikemoto et al., 1994) and exposure to high sulfide concentration (Rubio-Rincón et al., 2017a, 2017b; Saad et al., 2017),
52 interactions between sulfide, phosphate and iron in anaerobic digestion (Ge et al., 2013; Roussel and Carliell-Marquet,
53 2016), and the simultaneous sulfide oxidation and nitrate reduction known as autotrophic denitrification which has
54 been implied in the development of new processes e.g. SANI (Lau et al., 2006; Wang et al., 2009).

55 Sulfur in gaseous form is a challenge. Because of gaseous emission especially in form of H₂S, public concern has
56 arisen about WRRFs in the vicinity of residential areas (Frechen, 1988; Gostelow et al., 2001; Lebrero et al., 2013).
57 Consequently, the odour collection and treatment are becoming more and more required in WRRFs. H₂S emission
58 occurs in two categories of process units (Gostelow et al., 2001); process units that only promote emission of previously
59 formed H₂S e.g. wastewater inlet works and process units in which both formation and emission occur e.g. primary
60 settling/thickening. Based on information from literature, the two important sources of emission are primary treatments
61 and sludge treatment units (Dincer and Muezzinoglu, 2008; Jiang et al., 2017; Lebrero et al., 2011; Ras et al., 2008),
62 whereas the biological treatment units (aerobic, anoxic tanks and secondary settling) were shown to be less emissive
63 (Frechen, 2004).

64 Despite mentioned importance, less attention has been given to the sulfur cycle when it comes to full-scale studies.
65 What makes full-scale sulfur studies a challenging task might be the complexity of the sulfur cycle due to the
66 multiphase nature of sulfur (i.e. liquid, solid and gaseous states), a wide range of sulfur species and redox states,
67 ranging from sulfide (-2) to sulfate (+6), interrelated conversions and transformations and difficult sampling and
68 measurements especially for gaseous sulfur.

69 A key step towards enhancing sulfur studies in WRRFs is quantifying the distribution of sulfur in a plant-wide level
70 as it is helpful for: (i) identifying key sulfur flows, (ii) enabling quantitative comparison of sulfur flows in different
71 streams, (iii) identifying the influence of process units on sulfur flows, (iv) identifying key spots for sulfur recovery
72 and/or reducing the negative effects of sulfur and (v) facilitating the correct design of odour collection and treatment
73 facilities as data is typically scarce.

74 In literature, several studies partly addressed the distribution of sulfur flows in the sludge treatment units, providing
75 valuable information in regard to the effect of process units on the sulfur flows (Dewil et al., 2008, 2009; Fisher et al.,
76 2017; Yoshida et al., 2015). The role of secondary sludge thickening in reducing sulfur flows towards successive
77 process treatment was highlighted by Dewil et al. (2008, 2009), who traced flows of total sulfur through four WWTPs.
78 By mapping the sulfur flows in the sludge processing of six WWTPs with different configurations, Fisher et al. (2017)
79 noted higher sulfur recovery in sludge at sites with a combination of primary and secondary treatments, attributing it
80 to the incorporation of sulfate into the biomass and capturing and sending more solids to the sludge processing. Other
81 factors increasing sulfur recovery were higher efficiency of the primary settling tank, thickening and dewatering units,
82 as well as higher iron content in the digesters. Nevertheless, the comprehensive sulfur management in WRRFs requires

83 a plant-wide level approach as most process units are more or less affected by the sulfur cycle and because sulfur can
84 be distributed to water, sludge and gaseous streams.

85 In the process of tracking sulfur flows, Fisher et al. (2017) mentioned the limitations in data availability and quality,
86 which highlights the importance of thorough experimental design and data reconciliation for tracking substance flows
87 (Behnami et al., 2016; Meijer et al., 2002, 2015; Puig et al., 2008). To address this issue, Le et al. (2018) developed a
88 mass balanced-based experimental design procedure which provides Pareto-Optimal solutions (i.e. measurement
89 layouts) in terms of their cost and accuracy of key variables. These solutions guarantee the subsequent reconciliation
90 of the collected dataset through data reconciliation. Reconciliation, in this context, means that the value of variables,
91 regardless of being measured or not, would be calculated from other measurements based on the constraints in the
92 form of mass balances. This methodology is applied to a WRRF to trace sulfur flow to ensure the quality of data but
93 also prevent trivial measurements.

94 This study aims to quantify the distribution of sulfur flow in a municipal WRRF, addressing all process units in the
95 water line and sludge line as well as taking into account water, sludge and gaseous streams. The case study plant had
96 an innovative configuration in sludge treatment by having two-stage digestion with intermediate thermal treatment,
97 which enabled the evaluation of sludge post-treatment processes on sulfur flow distributions. The total sulfur mass
98 flows were obtained following three steps: experimental design, data collection and data reconciliation. The sulfur
99 flows throughout the plant were compared, identifying key flows and how they are influenced by unit processes.

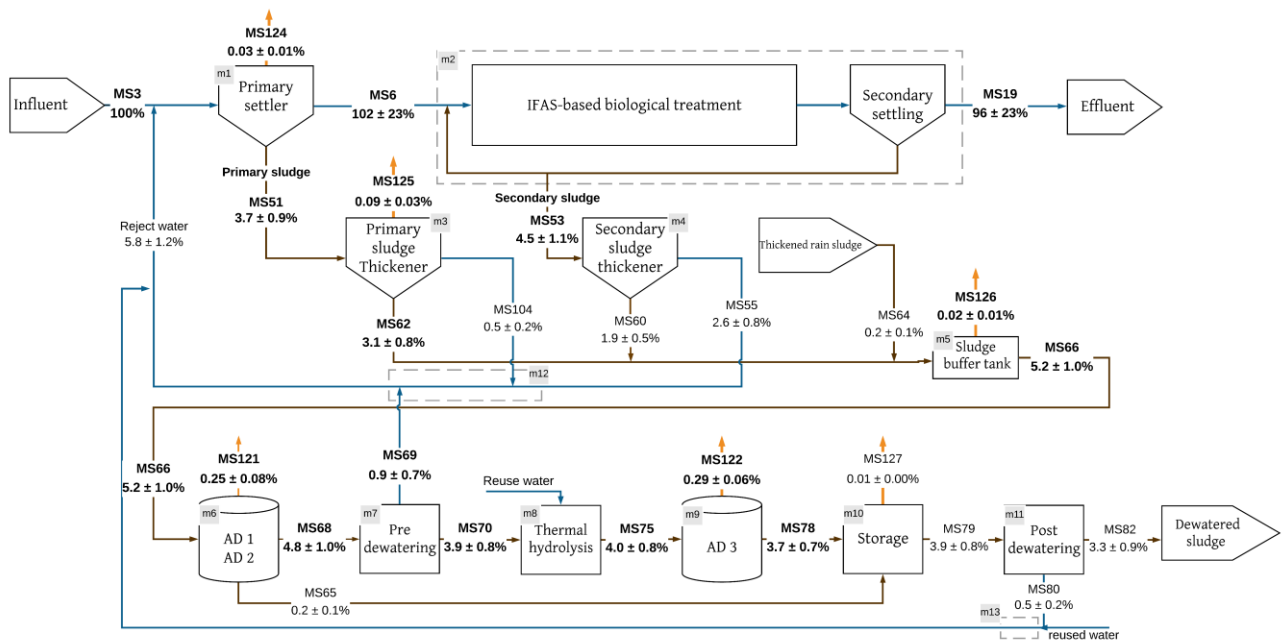
100 2. Material and methods

101 2.1. WRRF under study

102 The municipal WRRF under study (**Fig. 1**) has a capacity of 620,000 P.E. and comprises pre-treatment, secondary
103 treatment and sludge treatment. Pre-treatment process consists of screening and grit and grease removal, followed by
104 primary settling equipped with lamella plates. The primary settling effluent is sent to secondary treatment in an
105 integrated fixed-film activated sludge (IFAS) process for the removal of carbon, nitrogen and phosphorus. The
106 secondary treatment is realized in seven compartments: a pre-anoxic reactor, an anaerobic reactor, an anoxic reactor,
107 an aerated reactor with carriers, a de-oxygenation reactor without aeration, a post-anoxic reactor with methanol
108 addition and a post-aeration tank with aluminium chloride addition for chemical phosphorus removal. Effluent from

109 the secondary clarifier passes through filtration as a tertiary treatment before final discharge. During intense rain
110 events, the potential surplus influent wastewater flow is directed towards the rain treatment line which is based on
111 chemically enhanced primary treatment.

112 Primary and secondary sludge are pumped to the gravity thickener and dynamic thickener (rotary drums), respectively.
113 The thickened primary and secondary sludge as well as a small fraction of the thickened sludge originating from the
114 rain treatment line are mixed in a sludge buffer tank. Anaerobic digestion is performed in two stages, the first of which
115 takes place in two parallel units. The first-stage digested sludge is pre-dewatered by a centrifuge and sent to a thermal
116 hydrolysis unit (165°C, 8 bar, 30 minutes). The thermally treated sludge is diluted and cooled by adding some treated
117 effluent. The subsequent second stage digestion is performed in a single unit. All three digester tanks have the same
118 volume (6100 m³) and are equipped with air injection to the headspace for biological removal of hydrogen sulfide from
119 biogas (microaeration process). The second-stage digested sludge is sent to a storage tank and then dewatered by a
120 centrifuge. The filtrate of primary and secondary thickening, centrate of pre-dewatering and post-dewatering as well
121 as the reuse water, which is used for internal usages e.g. cleaning, return to the upstream of pre-treatment.



122

123 **Fig. 1:** Simplified process flow diagram of the WRRF under study. The total sulfur mass flows in the streams are
 124 given as a percentage of the total sulfur mass flow in the influent. Water streams, sludge streams and gas streams
 125 are shown in blue, brown and yellow lines, respectively. Key variables used in experimental design and data
 126 reconciliation are given in bold. The mass balances (#m) were derived around individual and/or combined process
 127 units; in the latter case, the boundaries are shown by dashed boxes.

128 **2.2. Measurement campaign**

129 The measurement campaign was performed during two weeks in June 2019. The measurement layout in this campaign
130 was selected by following an experimental design procedure (section 2.3.1). The sampling method in the water line
131 and sludge treatment lines were composite samples and grab samples, respectively. The water and sludge samples were
132 analysed for total sulfur ($\text{g S}\cdot\text{m}^{-3}$) using inductively coupled plasma optical emission spectrometry (ICP-OES)
133 following NF EN ISO 11885 standard. An overview of the measurements including the sampling points and the number
134 of samples is provided in section B2 in the Supplementary Information (SI).

135 Determination of gaseous sulfur from unit processes where high emission levels were expected was done by monitoring
136 the emitted hydrogen sulfide as the dominant gaseous sulfur species. Other volatile sulfur compounds in the gas phase
137 were assumed negligible, such that hydrogen sulfide was considered as an approximation of total sulfur in the gas
138 phase.

139 The studied process units included primary settler, primary thickener, sludge buffer tank, anaerobic digesters and
140 digested sludge storage tank. The data of sulfur mass flows in the biogas of anaerobic digesters were collected from
141 the supervisory control and data acquisition system (SCADA). In case of other process units, which were completely
142 covered, the myKlearSens H_2S meter (Klearios, France) and OdaLog[®] H_2S meters (App-Tek, Australia) were installed
143 on their ventilation pipes. Continuous measurements of gaseous H_2S were performed with a frequency of 5 minutes
144 over two weeks. In order to obtain the mass flow, air flow rates in the ventilation pipes were measured on the first day
145 of the campaign using pitot tube, hot-wire and helix anemometers. The flow rates of the water and sludge streams were
146 collected from the SCADA system.

147 **2.3. Quantification of total sulfur mass flows**

148 The main goal of this study was the quantification of the total sulfur flows in the WRRF. Experimental design was
149 applied to select sampling points that guaranteed obtaining a reliable and adequate data set through subsequent data
150 reconciliation. The experimental design and data reconciliation procedures were based on the principle of mass
151 conservation, the conservative quantity being total sulfur.

152 **2.3.1. Experimental design**

153 Experimental design was applied to choose the measurement layout to obtain the required information with a minimal
154 number of measurements and maximum accuracy. The step-wise experimental design procedure of Le et al. (2018)
155 (see section A1 in SI) was followed to this end. This experimental design procedure evaluates possible measurement
156 layouts through redundancy analysis and identifies the list of optimum solutions in terms of cost and accuracy that
157 guarantee the reconciliation of key variables. Reconciliation means that the value of key variables, regardless of being
158 measured or not, would be calculated from other measurements based on the constraints in the form of mass balances.
159 The applied experimental design procedure consists of 7 steps, which are detailed below.

160 As a first step, the main goal was translated into key variables, in this case 17 total sulfur mass flows (section A3 in
161 SI). The key variables covered water, sludge and gas lines and were selected as streams which were expected to contain
162 significant sulfur loads and/or to be involved in important sulfur conversions, based on information from literature and
163 expert knowledge. Gas streams which were expected to contain a significant amount of sulfur were added *a priori* as
164 measured variables (6 streams, see **Fig. 1** or **Table A5** in SI). Five of them were taken up as key variables (see **Table**
165 **A3** in SI). Second, mass balances for total sulfur flows were defined around individual and/or combined process units
166 (section A4 in SI). Third, data inventory was done based on historical data and expert knowledge to estimate the mean
167 values, expected uncertainties and the measurement cost of potential additionally measured variables (section A5 in
168 SI). The potential additional measured variables were limited to total sulfur concentrations. The flow rate
169 measurements were limited to ones already installed in the plant (30 out of 33 flows were measured). The experimental
170 design procedure then performed a redundancy analysis (step 4-6 of **Fig. A1** in SI) and solved a multi-objective
171 optimization problem (step7), minimising the cost (number of additional measurements) and maximizing the accuracy
172 (precision improvement of key variables). The results were visualised in a Pareto-optimal front that was used to select
173 the measurement layout.

174 **2.3.2. Data reconciliation**

175 The collected dataset was subject to the mass balance-based data reconciliation procedure of Le, (2019, see section B1
176 in SI). Provided there is sufficient redundancy in the dataset, this procedure provides better estimates for the key
177 variables in terms of their mean value and uncertainty. In addition, the applied procedure performs several gross error
178 detection techniques. The procedure can be divided into three steps, input preparation, data reconciliation and gross
179 error detection, which are detailed below.

180 The data reconciliation procedure required three input information, namely, key variables, mass balances and pre-
181 processing of the raw measurements. The key variables and mass balances were the same as for the experimental
182 design step. Pre-processing of the raw dataset involves listing the mean values and uncertainty of the measured
183 variables. Determination of variable uncertainties was done taking into account the measurement errors, standard error
184 and sampling method (see section B2 in SI).

185 The extent of data reconciliation was assessed based on two indicators, namely the correction factor and the precision
186 improvement. The correction factor (Δ_x) reflects the accuracy of measurements and is defined as the ratio of the
187 difference between the mean of the measurement ($mean(x)$) and the mean of the reconciled value ($mean(\bar{x})$) to the
188 mean of the measurement, expressed in percentage.

$$\Delta_x = \frac{mean(x) - mean(\bar{x})}{mean(x)} \quad \text{Eq.1}$$

189 The precision improvement (i_x), also known as the effect of balancing (van der Heijden et al., 1994), is defined as the
190 ratio of the difference between the variance of the measurement ($var(x)$) and the variance of the reconciled value
191 ($var(\bar{x})$) to the variance of the measurement, expressed in percentage. The higher the precision improvement, the
192 more accurate the value of the key variable is known after data reconciliation.

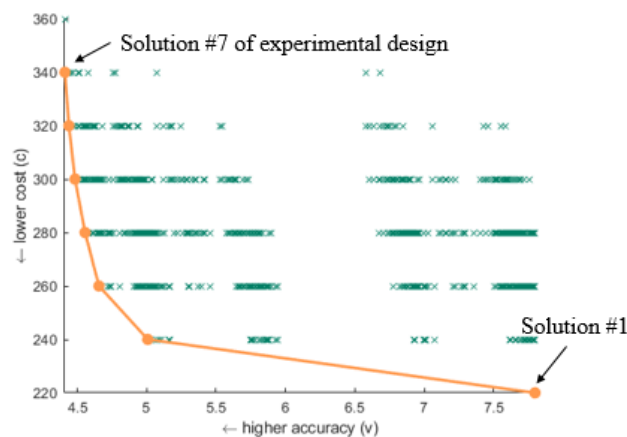
$$i_x = \frac{var(x) - var(\bar{x})}{var(x)} \times 100 \quad \text{Eq.2}$$

193 Furthermore, the dataset was checked for gross errors by testing the dataset against alternative hypotheses: (1) the null
194 hypothesis, H_0 , that no gross error is present, and (2) the alternative hypothesis, H_1 , that gross errors are present. Three
195 tests were incorporated in the data reconciliation procedure, namely, global test, nodal test and measurement test. The
196 global test provides a general signal if there is a potential gross error in the data set, the nodal test narrows this down
197 to individual constraints and the measurement test suggests potential suspected measurements with gross errors. Details
198 of these tests can be found in Le (2019).

200 3.1. Experimental design- selection of measurement layout

201 Key variables were selected from the water line, sludge line and gas streams (**Table A3** in SI). The experimental design
 202 evaluated whether or not the main goal, subsequent reconciliation of the key variables, was achievable for the given
 203 set of measurements and potential additionally measured variables (section A6 in SI). Based on the process flow sheet
 204 and the initially available measurements, 17 potentially additional sampling points for the measurement of total sulfur
 205 were identified, corresponding to $2^{17} = 1,310,072$ potential measurement layouts, i.e. combinations of potential
 206 additional sampling points. All measurement layouts were evaluated by the experimental design procedure. From all
 207 possible combinations, 3534 measurement layouts could result in the reconciliation of key variables and thus were
 208 considered as solutions, seven of them were optimal solutions, lying on the Pareto-front (**Fig. 2**, details of Pareto-
 209 Optimal solutions including the sampling points of each solution are given in section A6 in SI). Each of these solutions
 210 is a measurement layout that guarantees the improvement of defined key variables and is optimal in terms of cost and
 211 accuracy.

212 The Pareto-front groups the Pareto-optimal solutions meaning that a lower cost of measurements can only be obtained
 213 at the expense of lower accuracy of key variables and vice versa, higher accuracy can be obtained at the expense of a
 214 higher cost. Solution 1 was the cheapest measurement layout with 11 additional sampling points for the measurement
 215 of total sulfur concentration. Solution 7 with 17 additional measurements provided the highest accuracy and was
 216 selected as the measurement layout in this study.



218 **Fig. 2:** Solutions of experimental design. Solutions are expressed in terms of cost (c) and accuracy (v). Each x
219 represents a solution: the line filled circles represent the Pareto-front, containing all optimal solution.

220 Overall, the experimental design procedure proved successful in identifying Pareto-optimal measurement layouts,
221 balancing the number of measurements and their accuracy, despite handling the given relatively complex process
222 configuration including many possible sampling points.

223 **3.2. Data Reconciliation- Quality check**

224 A data quality check was performed for the water and, sludge streams, as well as for the gas streams. For each of them
225 correction factor, precision improvement, gross error detection was analysed.

226 **3.2.1. Water and sludge streams**

227 Data reconciliation results in reconciled (i.e. improved) values for key variables, which could be measured or
228 unmeasured variables. The measured key variables (total sulfur mass flows) in the water and sludge streams had
229 correction factors (Eq. 1) ranging from 1% to 15% (**Fig. 3a**). The maximum correction factors in the water line and
230 sludge line were seen in the influent wastewater (MS3) with an 8.7% increase in the value of raw measurement and
231 thickened primary sludge (MS62) with a 14.9% decrease in the raw measurement, respectively. This value for the feed
232 and digested sludge of the first stage digestion (MS66 and MS68) and second stage digestion (MS75 and MS78), which
233 have high retention time, was below 13%. Overall, the correction factors were low, reflecting that all imposed
234 constraints (mass balances) were met by small changes in the values of raw measurements. This indicates good
235 reliability of the raw measurements.

236 The total sulfur mass flow in the centrate of pre-dewatering (MS69) was an unmeasured key variable (i.e. both flow
237 and total sulfur concentration were unmeasured) for which the calculated mass flow from raw data was $15 \pm 92 \text{ kgS.d}^{-1}$
238 ¹ compared to $50 \pm 40 \text{ kgS.d}^{-1}$ from the reconciled data set that shows a 244% correction factor (data is given in section
239 B3 in SI).

240 The precision improvement (Eq. 2) of the key variables through data reconciliation, quantifying the reduction in
241 measurement uncertainty, is summarized in **Fig. 3b**. The average precision improvement of the key variables in the
242 water line and the sludge line was 72%. Total sulfur mass flow in the primary sludge (MS51) had the highest precision
243 improvement (96%). The uncertainty of the total sulfur mass flow in the primary sludge, which was defined as the

244 ratio of the standard error to the mean, was reduced significantly: from 79% in raw measurements to 19% in reconciled
245 value (section B3 in SI). Raw measurements from full-scale WRRFs bear uncertainties for various reasons, e.g.,
246 influent dynamics, sampling method and measurement errors. For instance, the significant variations in the total sulfur
247 concentrations in the primary sludge during the measurement campaign could be attributed to the different solid content
248 of the grab samples.

249 The precision improvement of measured variables by data reconciliation is beneficial for further data handling. This
250 improvement relies on redundancy in the measured data set that allowed variables to be estimated in several
251 independent ways from separate sets of constraints imposed by mass balances. The improvement of the standard
252 deviation of raw measurements by data reconciliation techniques was also reported for flow, COD and phosphorus in
253 literature (Behnami et al., 2016; Puig et al., 2008).

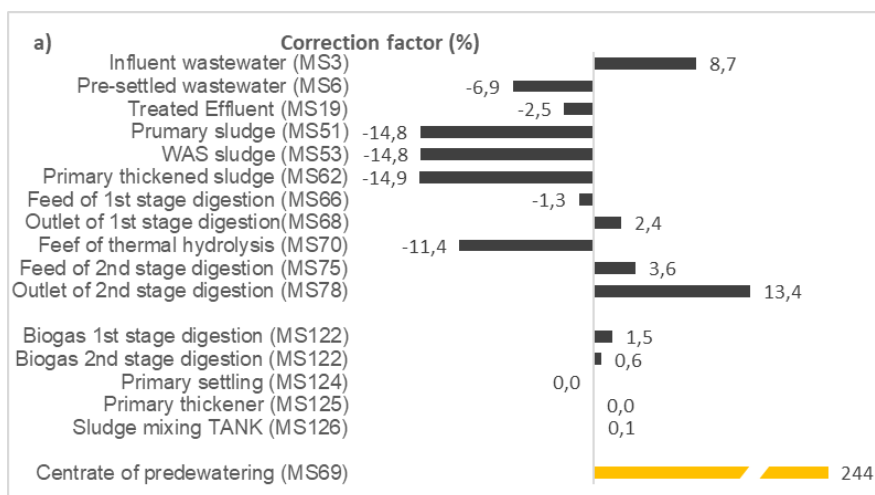
254 The global test, nodal test and measurement test detected no gross error in the total sulfur mass flows in the water line
255 and the sludge line. It is important to note that the high uncertainty of raw measurements (average of 26%) may
256 influence the detection of gross errors. However, in this case, there is an agreement between measured values and
257 reconciled values expressed through a low correction factor (15%).

258 3.2.2. Gas streams

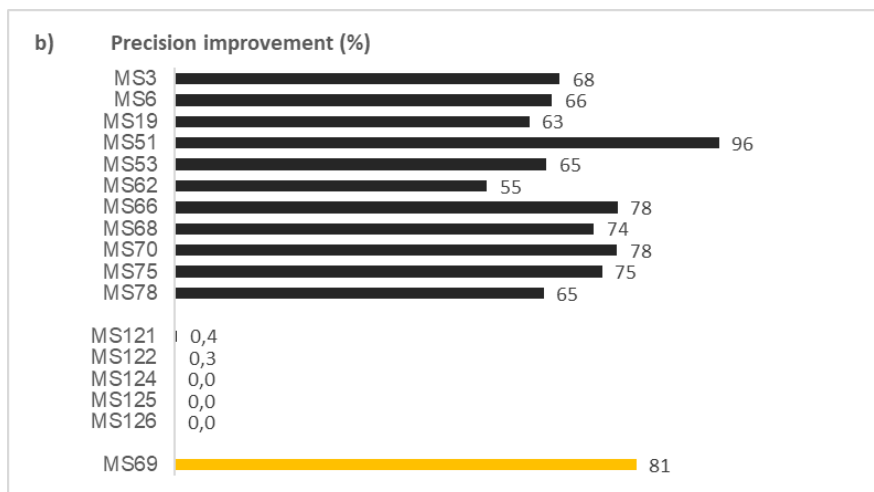
259 The values of the six measured gas streams are given in **Table B2** in SI. Five of them were key variables (MS121,
260 MS122, MS124, MS125, MS126), which means that their value was also reconciled, i.e., calculated from other
261 variables. However, their mean values and uncertainties hardly improved upon data reconciliation, the value of
262 correction factor and precision improvement being less than 1% (**Fig. 3a, 3b**). The very low precision improvement
263 indicates that data reconciliation did not really reconcile ('improve') these variables. The latter behaved as non-
264 redundant variables in the sense that their values could not be estimated from other sets of measurements in the mass
265 balances, even though they were indicated as redundant through the (theoretical) redundancy analysis. Such variables
266 are referred to as "practically non-redundant" (Narasimhan and Jordache, 1999). The reason why the total sulfur mass
267 flows in the gas streams were practically non-redundant in this study is because of their small mass flows compared to
268 those in the water and sludge streams. In case of primary settling, for instance, the sulfur flow in the gas stream
269 (MS124) and influent wastewater (MS3) were $2.0 \pm 0.5 \text{ kgS.d}^{-1}$ and $5817 \pm 947 \text{ kgS.d}^{-1}$, respectively (for more detail
270 see **Table B3** in SI). Indeed, the sulfur mass flows in gas streams were much smaller than the variance of the total
271 sulfur mass flows in water and sludge streams, which for the mentioned example is 2 orders of magnitude smaller.

272 Because of their practical non-redundancy, gross error detection could not be applied to the measurements of total
 273 sulfur in the gas phase. Still, the measurements in these gas streams were considered to be quite reliable because of the
 274 nature of the measurement: the units were covered and the air was extracted through a ventilation pipe, in which the
 275 H₂S analyser and the flow meter were installed. The reliability of the measurement is illustrated by the relatively low
 276 uncertainty range. For instance, the measured value of the total sulfur mass flow in the biogas of second stage digestion
 277 (MS122) was 16.9 ± 2.5 kgS.d⁻¹ (**Table B3** in SI). For comparison, if this variable would not have been measured but
 278 calculated from the available measurements and prevailing mass balances, its value would have been
 279 58.5 ± 50.1 kgS.d⁻¹, showing 85% uncertainty. Such high uncertainties, often above 100%, were also reported by
 280 Yoshida et al. (2015) when calculating the gaseous emissions from some process units in a conventional wastewater
 281 treatment plant were calculated from other measurements using mass balances. Similar results were also reported by
 282 Fisher et al. (2017) when calculating the total sulfur mass flows in the biogas of an anaerobic digester from total sulfur
 283 measurements in the feed and outlet of the digester.

284 Despite representing smaller mass flows, gaseous sulfur streams are very important due to the problems associated
 285 with emitted sulfur even in small quantities. They therefore need to be accurately determined by direct measurements
 286 rather than calculated from other measurements through mass balances. Indeed, it was shown in this study that gaseous
 287 sulfur streams cannot be accurately calculated through data reconciliation (i.e., do not qualify as key variables) because
 288 their values are very small compared to those of sulfur loads in the liquid and sludge streams.



289



290

291 **Fig. 3:** The indicators of data reconciliation a) Correction factor b) Precision improvement for quality check of the key
 292 variables. Measured key variables (black) and unmeasured key variables (yellow).

293 3.2.3. Effectiveness of experimental design and data reconciliation

294 In this work, the effectiveness of combining mass balance-based experimental design and data reconciliation
 295 procedures was demonstrated for the first time for reliable quantification of total sulfur flows and for a relatively
 296 complex WRRF. The Pareto-optimal measurement layouts put forward by the experimental design procedure showed
 297 valid for the identification of key variables. Data reconciliation and gross error detection provided better estimates for
 298 the total sulfur mass flows in the water line and the sludge line, fitting the total flow and total sulfur mass balances and
 299 characterized by a relatively high accuracy.

300 A balanced data set is a prerequisite for performing any type of process evaluation of full-scale water resource recovery
 301 facilities. Raw measurements are never fully accurate so the mass balances would not close perfectly without proper
 302 data reconciliation and gross error detection. For instance, model calibration and validation on erroneous data would
 303 lead to laborious and unjustified model calibrations of kinetics and stoichiometric parameters (Meijer, 2004). It is
 304 therefore, essential to reconcile the raw measurements to verify (gross) errors and improve their accuracy before being
 305 implemented.

306 3.3. Distribution of total sulfur mass flows

307 The plant-wide distribution of total sulfur mass flows using the reconciled data set is summarized in **Fig. 1**. In order to
 308 facilitate the comparison of streams, the total sulfur mass flows of the streams are expressed as the percentage of the

309 total sulfur mass flows in the influent wastewater (the absolute values are given in section B3 in SI). In what follows,
310 the total sulfur distribution in the water line, sludge line and gas streams is discussed consecutively.

311 **3.3.1. Sulfur distribution in the water line**

312 The influent wastewater (MS3, 100% total sulfur mass flow) is combined with the reject water from the sludge
313 treatment line $5.8 \pm 1.2\%$ and then enters the primary settling process (**Fig. 1**). Most of the total sulfur mass flow
314 entering primary settling remained in the water line with the pre-settled wastewater (MS6) accounting for $102 \pm 23\%$
315 of the total sulfur present in the influent. The high mass of sulfur in the pre-settled wastewater indicates that sulfur in
316 the influent wastewater is mostly in soluble form. This is in agreement with the findings of Dewil et al. (2008), who
317 reported that sulfate accounts for 99% of the sulfur in the influent wastewater.

318 After secondary treatment, comprising IFAS-based biological treatment (including anaerobic/anoxic/aerobic zones)
319 and secondary settling, the water stream (MS19) still comprised $96 \pm 23\%$ of the total sulfur mass flow in the incoming
320 wastewater (MS3). This is within the range of 78-98% reported by Fisher et al. (2017), including observations from
321 six wastewater treatment plants with different process configurations and influent wastewater flow rate. Overall, the
322 amount of total sulfur in the water line is hardly affected by conventional (secondary) water treatment processes. Still,
323 sulfur discharges through the dewatered sludge and gaseous emissions are critical because of their important impact
324 on (post-treatment) process operation.

325 **3.3.2. Sulfur distribution in the sludge line**

326 The primary sludge (MS51) and secondary sludge (MS53) streams contained about equal amounts of total sulfur mass
327 flows, amounting to $3.7 \pm 0.9\%$ and $4.5 \pm 1.1\%$ of the influent wastewater, respectively. In contrast, the distribution of
328 sulfur during thickening was different for primary and secondary sludge. In the primary thickener, the majority of
329 sulfur was directed to the thickened sludge (MS62, $3.1 \pm 0.8\%$) rather than filtrate (MS104, $0.5 \pm 0.2\%$), while the
330 secondary thickener resulted in a higher release of sulfur (57%) to the filtrate (MS55, $2.6 \pm 0.8\%$) compared to
331 thickened sludge (MS60, $1.9 \pm 0.5\%$). The long hydraulic retention time in the primary thickener (gravity thickening)
332 promoted the biological formation of sulfide, which may be emitted to the hydrogen sulfide or react with present metals
333 and form metal sulfide; hence reducing the soluble sulfur in the filtrate. As for the secondary sludge, soluble sulfur is
334 expected to be in the form of sulfate due to the redox conditions in the aeration zone as the last step of biological
335 treatment. Moreover, no significant microbial activity is expected in secondary thickener (rotary drums), in which

336 physical separation between liquid and solid forms would take place. Of the total sulfur mass flow entering secondary
337 thickening, 57% was directed to filtrate that is in agreement with the 50-68% values reported by Fisher et al. (2017).
338 A lower value (38%) was reported in the gravity belt thickener by Dewil et al. (2008). The direction of sulfur to filtrate
339 rather than the thickened sludge makes the dynamic thickener an important unit for reducing sulfur mass flows to the
340 subsequent sludge treatment units (e.g., anaerobic digestion) as was also concluded by (Dewil et al., 2008). Besides
341 thickened primary sludge and secondary sludge, the sludge buffer tank receives a fraction of thickened rain sludge
342 (MS64, $0.2 \pm 0.1\%$).

343 The contributions of different sludge sources, namely primary thickened sludge, secondary thickened sludge and
344 thickened rain sludge in terms of total sulfur flow to sludge buffer tank were about 60%, 36% and 4%, respectively. A
345 correlation between the primary sludge volatile solids content – as a source of organic sulfur in the form of
346 proteinaceous matter - and the hydrogen sulfide concentration in the biogas has been suggested by Erdirencelebi and
347 Kucukhemek (2018). This study strengthens their findings through the quantification of the total sulfur flow in the
348 primary thickened sludge, which clearly represents a considerable contribution to anaerobic digestion.

349 During the first stage digestion, the total sulfur mass flow decreased from $5.2 \pm 1.0\%$ in the feed to $4.8 \pm 1.0\%$ in the
350 digested sludge, implying that sulfur mostly remained in the digested sludge. Other studies have not detected
351 significant flows of sulfur in the biogas during the studying of sulfur flows in anaerobic digestion (Dewil et al., 2008;
352 Du and Parker, 2013; Yoshida et al., 2015). During the digestion process, the formation of insoluble sulfide and
353 hydrogen sulfide are expected due to the reduction of sulfate and also degradation of organic sulfur especially from
354 primary sludge source (Du and Parker, 2013). Sulfur removed in the centrate following the pre-dewatering of the
355 anaerobically digested sludge (MS69) was $0.9 \pm 0.7\%$ of the sulfur in the influent wastewater, showing that 18% sulfur
356 entering pre-dewatering process being removed in the centrate. Fisher et al. (2017) reported the range of 0.5-23.1%
357 and the range was attributed to different solid separation efficiencies of the dewatering processes. On the other hand,
358 other studies noted minimal sulfur in the centrate of the dewatering process that was explained by the formation of
359 insoluble metal sulfide complexes in the anaerobic digester (Dewil et al., 2008; Yoshida et al., 2015).

360 Despite a small increase in the mass of sulfur during thermal hydrolysis, which was due to the addition of reuse water
361 containing sulfur, the total sulfur mass flow during the thermal hydrolysis remained the same with $3.9 \pm 0.8\%$ and
362 $4.0 \pm 0.8\%$ sulfur mass flow in the feed (MS70) and outlet (MS75) of this unit, respectively. Liu et al. (2015) studied
363 the release of sulfur-containing odorants during the pyrolysis of sewage sludge and noted that the formation of H_2S ,
364 the predominant odorant, at $150^\circ C$ was insignificant. Although not yet addressed in the literature, the solubilisation of

365 organic sulfur during thermal hydrolysis may promote the formation and emission of hydrogen sulfide to the biogas
366 of subsequent anaerobic digestion.

367 Sulfur mass flow in the second stage of anaerobic digestion following thermal hydrolysis decreased from $4.0 \pm 0.8\%$
368 in the feed (MS75) to $3.7 \pm 0.7\%$ in the digested sludge (MS78). This implies that 7% of the sulfur in the feed of
369 second-stage digestion unit ends up in the biogas, which is considerable. The further reduction in the total sulfur flow
370 in the sludge line through second-stage digestion is particularly interesting knowing that the degradation of sulfur
371 species already occurred during the first-stage digestion, which indicates a possible effect of sludge thermal treatment.
372 The hydrolysis of organic material during thermal hydrolysis especially in case of organic sulfur present in the protein
373 of biomass. According to Du and Parker (2013), a small fraction of protein in secondary sludge, which are likely the
374 major contributors of organic sulfur in these streams, are not very well biodegradable in anaerobic digestion, so it could
375 be that this source of sulfur was not degraded during the first stage digestion. While proteins are protected from the
376 enzymatic hydrolysis during anaerobic digestion by the cell wall, thermal pre-treatment destroys the cell walls and
377 makes the proteins accessible for biological degradation (Neyens and Baeyens, 2003). In another study, Bougrier et al.
378 (2008) noted strong solubilisation of protein (95%) during thermal hydrolysis at 170°C and Brooks (1970) reported
379 40-60% solubilisation of organic material. Therefore, elimination of the rate-limiting factor in anaerobic digestion, i.e.
380 hydrolysis, (Wilson and Novak, 2009) and the cell destruction might explain the increasing removal of sulfur in the
381 second stage digestion.

382 The total sulfur mass flows removed through the centrate of post-dewatering (MS80) units was $0.5 \pm 0.2\%$, showing
383 13.6% sulfur removal through centrate of post-dewatering. This high sulfur removal was due to the solubilisation of
384 sulfur happening during thermal hydrolysis. Overall, the total sulfur mass flow in the reject water i.e., the centrates of
385 primary sludge and secondary sludge thickening, pre-dewatering and post-dewatering processes, accounted for
386 $5.8 \pm 1.2\%$ of the sulfur mass flow in incoming wastewater. The amount of total sulfur mass flow in the post-dewatered
387 sludge (MS82) was $3.3 \pm 0.9\%$ of the total sulfur in the influent wastewater.

388 The unique configuration of the two-stage anaerobic digestions with intermediate pre-dewatering, thermal hydrolysis
389 and post-dewatering in the case study plant caused a 36% decrease in the total sulfur mass flow. Lower sulfur content
390 in the dewatered sludge is desirable especially when the sludge is further used for co-combustion with other fuels in
391 power stations or cement kilns, or incineration in dedicated sludge combustors because lower sulfur dioxide (SO_2) is
392 emitted with the fuel gases (Van de Velden et al., 2008; Werther and Ogada, 1999).

393 3.3.3. Gaseous sulfur streams

394 The amount of H₂S gas streams monitored in this study accounted for $0.7 \pm 0.1\%$ of the total sulfur mass flows in the
395 influent wastewater (**Fig. 1**). Despite representing only small fractions of the total sulfur load, H₂S emissions are critical
396 because they cause odour nuisance, lower biogas quality and corrosion. Of the total gaseous sulfur emissions, 78%
397 were related to the biogas of the first stage and the second stage digestion and 22% from fugitive emissions during
398 primary settling, primary thickening, sludge buffer tank and digested sludge storage tank. Note that only the H₂S
399 emissions from these process units were measured, the H₂S emission from other process units such as biological
400 treatment was assumed negligible. No significant odour was detected in the biological treatment and clarifiers during
401 the measurement campaign which supports previous studies that showed the lowest emission from these units (Frechen,
402 2004). Nevertheless, while previous studies were merely qualitative (based on odour emissions), this study enabled
403 the full quantification of gaseous sulfur emissions and their comparison.

404 The majority of H₂S mass flow was detected in the second stage digestion (MS122, $0.29 \pm 0.06\%$) and first stage
405 digestion (MS121, $0.25 \pm 0.08\%$), which accounted for 78% of the total mass of emitted H₂S. The high mass flow of
406 gaseous H₂S in the second-stage digestion is in line with the abovementioned potential effect of sludge thermal
407 treatment on H₂S formation.. Two other emissive process units were primary thickener (MS125) and primary settling
408 (MS124) with $0.03 \pm 0.01\%$ and $0.09 \pm 0.03\%$ of the total sulfur mass flows in the influent, respectively. The long
409 hydraulic retention time (HRT) of the primary thickener and reductive conditions promotes the formation and
410 subsequent emission of gaseous sulfur which was also accompanied by a drop in the ORP and pH of the samples taken
411 from thickened sludge. The mass of emitted sulfur from sludge buffer tank (MS126) was $0.02 \pm 0.01\%$. It was expected
412 to have more emission due to the presence of biomass from thickened secondary sludge that could increase the
413 reduction of remained sulfate and organic sulfur. One explanation could be the presence of iron in the thickened rain
414 sludge which might lead to the formation of FeS and thus less sulfur in gas streams. The lowest sulfur flow to the gas
415 streams was detected in the digested sludge storage tank (MS127) with 0.01%.

416 3.4. Implications for research and practice

417 In this work, a thorough investigation of total sulfur flows was performed, identifying key sulfur flows over individual
418 unit processes in a plant-wide context and pointing out their relative importance. The large majority of sulfur mass
419 flow in the influent (96 ± 23) left the plant through the treated effluent. The sulfur in dewatered sludge accounted for
420 $3.3 \pm 0.9\%$, while gaseous emissions amounted to $0.7 \pm 0.1\%$. Despite forming a small portion of total sulfur flow,

421 the gaseous sulfur flows are highly undesirable and therefore require collection and treatment prior to release to the
422 atmosphere or utilisation of biogas in co-generation.

423 The detailed quantification of gaseous streams showed that most (gaseous) H₂S emissions, namely 42% of total H₂S
424 emission, were produced in the second-stage anaerobic digester, ending up in the biogas. The higher H₂S emissions
425 from the second-stage digester compared to first stage (35.7%) suggests an impact of thermal treatment on the
426 production of H₂S. Further investigation on the mechanisms and conversion of sulfur species –organic and inorganic
427 species– are required for understanding this trend and applying control techniques as high H₂S flows reduce the quality
428 of biogas and cause corrosion problems on downstream equipment. H₂S was also produced in the primary thickener
429 (13.5%) and the primary settler (4.9%). The relatively high H₂S emissions from the primary (gravity) thickener
430 suggests the formation and emission of hydrogen sulfide during relatively long hydraulic retention time. In view of
431 accurately modelling H₂S emissions, H₂S formation under anaerobic conditions thus needs to be considered to
432 overcome the limitation of currently available H₂S emission models (Santos et al., 2013).

433 When the treated sludge is used for combustion, it is beneficial to have low sulfur content in view of SO₂ formation
434 upon combustion. In this regard, the secondary (drum) thickener proved effective for limiting sulfur flows towards the
435 subsequent sludge treatment by directing majority of entering sulfur flows towards the centrate. Sludge treatment
436 through two-stage digestion configuration with intermediate thermal hydrolysis and pre and post dewatering also
437 considerably reduced (by 36%) the total sulfur content remained in dewatered sludge.

438 **4. Conclusions**

439 Sulfur mass flows in a full-scale water resource recovery facility (WRRF) were quantified for the first time on a plant-
440 wide level, assessing liquid, sludge and gas streams simultaneously.

- 441 - Total sulfur was demonstrated to be a conservative quantity, allowing the reliable quantification of total sulfur
442 flows through mass balance-based experimental design and data reconciliation procedures.
- 443 - The water treatment line hardly affected the incoming sulfur flows as sulfur was mostly removed through the
444 treated effluent. Amounting to about 8% of the sulfur in the influent wastewater, the sulfur flows in the
445 primary and secondary sludge caused high H₂S emissions in primary thickener and in both stages of anaerobic
446 digestion. In particular, the relatively higher H₂S emissions from the second-stage digester suggested an
447 impact of the thermal treatment resulting in increased H₂S production.

448 - Gaseous sulfur loads representing a relatively low mass are non-redundant in practice, which means that their
449 values cannot be accurately determined from measured variables and mass balances. Gaseous H₂S emissions
450 therefore need to be measured directly for obtaining reliable data.

451 5. Acknowledgements

452 This work was performed within the framework of the EUR H2O' Lyon (ANR-17-EURE-0018) of Université de Lyon
453 (UdL), within the program "Investissements d'Avenir" operated by the French National Research Agency (ANR). The
454 work of Kimberly Solon was supported by the Research Foundation Flanders (FWO) through an ERC runner-up
455 project for Eveline Volcke and by European Union's Horizon 2020 research and innovation programme under the
456 Marie Skłodowska-Curie Grant Agreement No. 846316 (WISEFLOW). The authors thank Sylvain Chastresse,
457 Christophe Renner, Jonathan Coulmin, Vanessa Gromand, Ian Garcia-Fernandez from Veolia for facilitating and
458 carrying out the measurement campaign.

459 6. References

- 460 Appels, L., Baeyens, J., Degrève, J., Dewil, R., 2008. Principles and potential of the anaerobic digestion of waste-
461 activated sludge. *Prog. energy Combust. Sci.* 34, 755–781.
- 462 Baetens, D., Weemaes, M., Hosten, L., De Vos, P., Vanrolleghem, P.A., 2001. Enhanced Biological Phosphorus
463 Removal Competition and symbiosis between SRBs and PAOs on lactateacetate feed. *J. Exp. Bot.* 57, 3813–
464 3824.
- 465 Behnami, A., Shakerkhatibi, M., Dehghanzadeh, R., Benis, K.Z., Derafshi, S., Fatehifar, E., 2016. The implementation
466 of data reconciliation for evaluating a full-scale petrochemical wastewater treatment plant. *Environ. Sci. Pollut.*
467 *Res.* 23, 22586–22595.
- 468 Bougrier, C., Delgenès, J.P., Carrère, H., 2008. Effects of thermal treatments on five different waste activated sludge
469 samples solubilisation, physical properties and anaerobic digestion. *Chem. Eng. J.* 139, 236–244.
470 <https://doi.org/10.1016/j.cej.2007.07.099>
- 471 Brooks, R., 1970. Heat treatment of sewage sludge. *Water Pollut Contr (London)* 69, 92–99.
- 472 Chen, Y., Cheng, J.J., Creamer, K.S., 2008. Inhibition of anaerobic digestion process: a review. *Bioresour. Technol.*
473 99, 4044–4064.
- 474 Dewil, R., Baeyens, J., Roels, J., Steene, B. Van De, 2009. Evolution of total sulphur content in full scale wastewater
475 sludge treatment. *Environ. Eng. Sci.* 26, 292–300.
- 476 Dewil, R., Baeyens, J., Roels, J., Steene, B. Van De, 2008. Distribution of sulphur compounds in sewage sludge
477 treatment. *Environ. Eng. Sci.* 25, 879–886.
- 478 Dincer, F., Muezzinoglu, A., 2008. Odor-causing volatile organic compounds in wastewater treatment plant units and
479 sludge management areas, in: *Journal of Environmental Science and Health - Part A Toxic/Hazardous*
480 *Substances and Environmental Engineering.* Taylor & Francis, pp. 1569–1574.
- 481 Du, W., Parker, W., 2013. Characterization of sulfur in raw and anaerobically digested municipal wastewater treatment

- 482 sludges. *Water Environ. Res.* 85, 124–132.
- 483 Erdirencelebi, D., Kucukhemek, M., 2018. Control of hydrogen sulphide in full-scale anaerobic digesters using iron
484 (III) chloride: Performance, origin and effects. *Water SA* 44, 176–183.
- 485 Fisher, R.M., Alvarez-Gaitan, J.P., Stuetz, R.M., Moore, S.J., 2017. Sulfur flows and biosolids processing: using
486 Material Flux Analysis (MFA) principles at wastewater treatment plants. *J. Environ. Manage.* 198, 153–162.
- 487 Frechen, F.-B., 2004. Odour emission inventory of German wastewater treatment plants-odour flow rates and odour
488 emission capacity. *Water Sci. Technol.* 50, 139–146.
- 489 Frechen, F.B., 1988. Odour emissions and odour control at wastewater treatment plants in West Germany. *Water Sci.*
490 *Technol.* 20, 261–266.
- 491 Galloway, J.N., Cowling, E.B., 2002. Reactive nitrogen and the world: 200 years of change. *AMBIO A J. Hum.*
492 *Environ.* 31, 64–71.
- 493 Ge, H., Zhang, L., Batstone, D.J., Keller, J., Yuan, Z., 2013. Impact of iron salt dosage to sewers on downstream
494 anaerobic sludge digesters: sulfide control and methane production. *J. Environ. Eng.* 139, 594–601.
- 495 Gostelow, P., Parsons, S.A., Stuetz, R.M., 2001. Odour measurements for sewage treatment works. *Water Res.* 35,
496 579–597.
- 497 Guerrero, L., Montalvo, S., Huiliñir, C., Campos, J.L., Barahona, A., Borja, R., 2016. Advances in the biological
498 removal of sulphides from aqueous phase in anaerobic processes: A review. *Environ. Rev.* 24, 84–100.
- 499 Guest, J.S., Skerlos, S.J., Barnard, J.L., Beck, M.B., Daigger, G.T., Hilger, H., Jackson, S.J., Karvazy, K., Kelly, L.,
500 Macpherson, L., 2009. A new planning and design paradigm to achieve sustainable resource recovery from
501 wastewater. *Environ. Sci. Technol.* 43, 6126–6130.
- 502 Gutierrez, O., Park, D., Sharma, K.R., Yuan, Z., 2010. Iron salts dosage for sulfide control in sewers induces chemical
503 phosphorus removal during wastewater treatment. *Water Res.* 44, 3467–3475.
- 504 Hao, X., Wang, X., Liu, R., Li, S., van Loosdrecht, M.C.M., Jiang, H., 2019. Environmental impacts of resource
505 recovery from wastewater treatment plants. *Water Res.* 160, 268–277.
- 506 Harada, H., Uemura, S., Momonoi, K., 1994. Interaction between sulfate-reducing bacteria and methane-producing
507 bacteria in UASB reactors fed with low strength wastes containing different levels of sulfate. *Water Res.* 28,
508 355–367.
- 509 Jiang, G., Melder, D., Keller, J., Yuan, Z., 2017. Odor emissions from domestic wastewater: a review. *Crit. Rev.*
510 *Environ. Sci. Technol.* 47, 1581–1611.
- 511 Lau, G.N., Sharma, K.R., Chen, G.H., Van Loosdrecht, M.C.M., 2006. Integration of sulphate reduction, autotrophic
512 denitrification and nitrification to achieve low-cost excess sludge minimisation for Hong Kong sewage. *Water*
513 *Sci. Technol.* 53, 227–235.
- 514 Le, H.Q., 2019. *Mass-Balance-based Experimental Design and Data Reconciliation for Wastewater Treatment*
515 *Processes*. Ghent University.
- 516 Le, Q.H., Verheijen, P.J.T., van Loosdrecht, M.C.M., Volcke, E.I.P., 2018. Experimental design for evaluating WWTP
517 data by linear mass balances. *Water Res.* 142, 415–425.
- 518 Lebrero, R., Bouchy, L., Stuetz, R., Muñoz, R., 2011. Odor assessment and management in wastewater treatment
519 plants: a review. *Crit. Rev. Environ. Sci. Technol.* 41, 915–950.
- 520 Lebrero, R., Rangel, M.G.L., Muñoz, R., 2013. Characterization and biofiltration of a real odorous emission from
521 wastewater treatment plant sludge. *J. Environ. Manage.* 116, 50–57.
- 522 Liu, S., Wei, M., Qiao, Y., Yang, Z., Gui, B., Yu, Y., Xu, M., 2015. Release of organic sulfur as sulfur-containing

- 523 gases during low temperature pyrolysis of sewage sludge. *Proc. Combust. Inst.* 35, 2767–2775.
- 524 Lomans, B.P., Drift, C. Van Der, Pol, A., Camp, H.J.M.O. Den, van der Drift, C., Pol, A., Op den Camp, H.J.M., 2002.
525 Cellular and molecular life sciences microbial cycling of volatile organic sulfur compounds. *Cell. Mol. Life Sci.*
526 59, 575–588.
- 527 Marti, N., Ferrer, J., Seco, A., Bouzas, A., 2008. Optimisation of sludge line management to enhance phosphorus
528 recovery in WWTP. *Water Res.* 42, 4609–4618.
- 529 Meijer, S.C.F., Van Der Spoel, H., Susanti, S., Heijnen, J.J., Van Loosdrecht, M.C.M., 2002. Error diagnostics and
530 data reconciliation for activated sludge modelling using mass balances, in: *Water Science and Technology*. pp.
531 145–156.
- 532 Meijer, S.C.F., 2004. Theoretical and practical aspects of modelling activated sludge processes.
- 533 Meijer, S.C.F., van Kempen, R.N.A., Appeldoorn, K.J., 2015. Plant upgrade using big-data and reconciliation
534 techniques, in: *Applications of Activated Sludge Models*. pp. 357–410.
- 535 Mihelcic, J.R., Fry, L.M., Shaw, R., 2011. Global potential of phosphorus recovery from human urine and feces.
536 *Chemosphere* 84, 832–839.
- 537 Muyzer, G., Stams, A.J.M., 2008. The ecology and biotechnology of sulphate-reducing bacteria. *Nat. Rev. Microbiol.*
538 6, 441–454.
- 539 Narasimhan, S., Jordache, C., 1999. *Data Reconciliation and Gross Error Detection, Data Reconciliation and Gross
540 Error Detection*. Elsevier.
- 541 Neyens, E., Baeyens, J., 2003. A review of thermal sludge pre-treatment processes to improve dewaterability. *J.*
542 *Hazard. Mater.* 98, 51–67.
- 543 Puchongkawarin, C., Gomez-Mont, C., Stuckey, D.C., Chachuat, B., 2015. Optimization-based methodology for the
544 development of wastewater facilities for energy and nutrient recovery. *Chemosphere* 140, 150–158.
- 545 Puig, S., van Loosdrecht, M.C.M., Colprim, J., Meijer, S.C.F., 2008. Data evaluation of full-scale wastewater treatment
546 plants by mass balance. *Water Res.* 42, 4645–4655.
- 547 Puyol, D., Batstone, D.J., Hülsen, T., Astals, S., Peces, M., Krömer, J.O., 2017. Resource recovery from wastewater
548 by biological technologies: Opportunities, challenges, and prospects. *Front. Microbiol.* 7, 1–23.
- 549 Ras, M.R., Borrull, F., Marcé, R.M., 2008. Determination of volatile organic sulfur compounds in the air at sewage
550 management areas by thermal desorption and gas chromatography–mass spectrometry. *Talanta* 74, 562–569.
- 551 Roussel, J., Carliell-Marquet, C., 2016. Significance of vivianite precipitation on the mobility of iron in anaerobically
552 digested sludge. *Front. Environ. Sci.* 4, 60.
- 553 Rubio-Rincón, F.J., Lopez-Vazquez, C.M., Welles, L., Van Loosdrecht, M.C.M., Brdjanovic, D., 2017a. Sulphide
554 effects on the physiology of *Candidatus Accumulibacter phosphatis* type I. *Appl. Microbiol. Biotechnol.* 101,
555 1661–1672.
- 556 Rubio-Rincón, F.J., Welles, L., Lopez-Vazquez, C.M., Nierychlo, M., Abbas, B., Geleijnse, M., Nielsen, P.H., Van
557 Loosdrecht, M.C.M., Brdjanovic, D., 2017b. Long-term effects of sulphide on the enhanced biological removal
558 of phosphorus: the symbiotic role of *Thiothrix caldifontis*. *Water Res.* 116, 53–64.
- 559 Saad, S.A., Welles, L., Lopez-Vazquez, C.M., van Loosdrecht, M.C.M., Brdjanovic, D., 2017. Sulfide effects on the
560 anaerobic metabolism of polyphosphate-accumulating organisms. *Chem. Eng. J.* 326, 68–77.
- 561 Santos, J.M., Sa, L.M. de, Reis Junior, N.C., Horan, N.J., 2013. Kinetic models of hydrogen sulphide formation in
562 anaerobic bioreactors. *Environ. Technol. Rev.* 2, 45–54.
- 563 Schippers, A., Jørgensen, B.B., 2002. Biogeochemistry of pyrite and iron sulfide oxidation in marine sediments.

- 564 Geochim. Cosmochim. Acta 66, 85–92.
- 565 Solon, K., Jia, M., Volcke, E.I.P., 2019a. Process schemes for future energy-positive water resource recovery facilities.
566 Water Sci. Technol. 79, 1808–1820.
- 567 Solon, K., Volcke, E.I.P., Spérandio, M., van Loosdrecht, M.C.M., 2019b. Resource recovery and wastewater
568 treatment modelling. Environ. Sci. Water Res. Technol. 5, 631–642.
- 569 Tchobanoglous, G., Burton, F., Stensel, H.D., 2003. Wastewater engineering: Treatment and reuse. Am. Water Work.
570 Assoc. J. 95, 201.
- 571 Van de Velden, M., Dewil, R., Baeyens, J., Jossion, L., Lanssens, P., 2008. The distribution of heavy metals during
572 fluidized bed combustion of sludge (FBSC). J. Hazard. Mater. 151, 96–102.
- 573 van der Heijden, R.T.J.M., Heijnen, J.J., Hellinga, C., Romein, B., Luyben, K.C.A.M., 1994. Linear constraint relations
574 in biochemical reaction systems: I. Classification of the calculability and the balanceability of conversion rates.
575 Biotechnol. Bioeng. 43, 3–10.
- 576 Visser, A., Beeksmas, I., Van der Zee, F., Stams, A.J.M., Lettinga, G., 1993. Anaerobic degradation of volatile fatty
577 acids at different sulphate concentrations. Appl. Microbiol. Biotechnol. 40, 549–556.
- 578 Wang, J., Lu, H., Chen, G.-H., Lau, G.N., Tsang, W.L., van Loosdrecht, M.C.M., 2009. A novel sulfate reduction,
579 autotrophic denitrification, nitrification integrated (SANI) process for saline wastewater treatment. Water Res.
580 43, 2363–2372.
- 581 Wanner, J., Kucman, K., Ottova, V., Grau, P., 1987. Effect of anaerobic conditions on activated sludge filamentous
582 bulking in laboratory systems. Water Res. 21, 1541–1546.
- 583 Werther, J., Ogada, T., 1999. Sewage sludge combustion. Prog. energy Combust. Sci. 25, 55–116.
- 584 Wilson, C.A., Novak, J.T., 2009. Hydrolysis of macromolecular components of primary and secondary wastewater
585 sludge by thermal hydrolytic pretreatment. Water Res. 43, 4489–4498.
- 586 Yamamoto-Ikemoto, R., Matsui, S., Komori, T., 1994. Ecological interactions among denitrification, poly-P
587 accumulation, sulfate reduction, and filamentous sulfur bacteria in activated sludge. Water Sci. Technol. 30, 201.
- 588 Yang, G., Zhang, G., Zhuan, R., Yang, A., Wang, Y., 2016. Transformations, inhibition and inhibition control methods
589 of sulfur in sludge anaerobic digestion: a review. Curr. Org. Chem. 20, 2780–2789.
- 590 Yoshida, H., Christensen, T.H., Guildal, T., Scheutz, C., 2015. A comprehensive substance flow analysis of a
591 municipal wastewater and sludge treatment plant. Chemosphere 138, 874–882.